# Percolation in a self-avoiding vortex gas model of the λ transition in three dimensions

James H. Akao*
*Institute for Advanced Study, Olden Lane, Princeton, New Jersey 08540*
(Received 31 October 1995)

A Monte Carlo simulation of the equilibria of a three-dimensional gas of vortex loops is conducted. Lines of vorticity are expressed as closed self-avoiding walks on a lattice. Vortices interact at low temperatures through a Biot-Savart potential arising through the Villian approximation of the $XY$ action. The vortex model at infinite temperature is also related to Symanzik's random-loop expansion of the critical $XY$ model. The low-temperature state of the model simulates thermally excited vorticity in superfluid helium. The high temperature state of the vortex gas has application to classical turbulence. A grand-canonical ensemble is simulated, in which chemical potential is a parameter related to the self-energy per unit length of a vortex line. Two phases are identified in the temperature–chemical potential plane; the phases are separated by a transition line analogous to the λ transition of superfluid helium. The transition line is also a percolation threshold; all vortex loops are of finite size in the cold phase, while an infinite vortex loop exists in the hot phase. The percolation transition driven by chemical potential persists to infinite temperature. At the infinite temperature ''polymeric'' state the Biot-Savart interaction vanishes and the behavior of the system is determined only by the density of vortices and geometric constraints. [S1063-651X(96)08206-2]

PACS number(s): 47.32.Cc, 64.60.Cn, 67.40.Vs, 05.50.+q

## I. INTRODUCTION

The relationship in fluid dynamics between small-scale motions and bulk flow properties is of great scientific and practical interest. Microscopic vortices dissipate energy in superfluid helium [1–3], and a gas of thermally excited vortices is identified with the ''normal component'' of liquid helium below the λ temperature. Vortex structure also plays a role in models of turbulence in classical fluids [4–6].

While the dynamics of superfluid and of turbulent flows are exceedingly complex, the small space and time scales are assumed to be universal. These scales should be described by a measure that is approximately invariant under the dynamics [7]. While little is rigorously known of the measure for classical turbulence, thermodynamic equilibria in vorticity variables [8–11] have been proposed as candidate measures.

In superfluid turbulence, quantized vorticity can interact with boundaries and with other excitations in such a way as to reach an equilibrium state. Proliferating vortex tangles are believed to play a role in disordering the condensate in superfluids [12] and superconductors [13]. Models of vortex equilibria give rise to theories of the helium λ transition [14–16].

While two-dimensional vortex models of superfluid helium are well described by the Kosterlitz-Thouless theory [17–19], the vortex structure in the three-dimensional models is not fully understood. The geometry of vortex lines in three dimensions affects both the energy and the entropy of the system. Large-scale vortices have been conjectured to resemble self-avoiding walks [14] at the λ transition. Studies also indicate that the connectivity of vortices influences the thermodynamics [20] of the system.

A complete vortex theory of the λ transition should be consistent with the behavior of the three-dimensional $XY$ model at the ordering transition. Critical exponents derived for vortex models can be compared with those of the $XY$ model to investigate the validity of theories. The exponents for the $XY$ model are available to high accuracy from $\epsilon$ expansion techniques, and are in good agreement with superfluid experiment [21].

The energy of an $XY$ spin configuration can be expressed through a low-temperature approximation [22,23] as a spin-wave term plus a vortex term arising from topological defects in the spin field. Monte Carlo simulations of the three-dimensional $XY$ model resolving topological defects in the spin field [24,25] demonstrate that vortex excitations proliferate with increasing temperature and are necessary to disorder the system. Suggestions about a general treatment of $XY$ vortices are given in [26].

Vorticity based theories of the ordering transition simplify vortex-vortex interaction energies and neglect spin waves. A computational simulation that employs these approximations provides a comparison with the spin-defect calculations. Vorticity simulation can thus be used to validate vortex equilibrium models of the λ transition. A complete equilibrium theory could then be extended to nonequilibrium problems of superfluid flow. Vortex statistics also play a central role in flux-line modeling of superconductors [27,28]. Aspects of superfluid vorticity simulation could also be employed in superconductor simulation.

This paper presents the results of a simulation of a gas of vortices in which vortex lines are the primitive variables rather than the defects of a spin field. A phase transition is identified in which the energy remains finite but the specific heat diverges or has a cusp. The transition is shown to be a percolation threshold; while the vortex line density is continuous across the transition, the probability of an infinite vortex loop forming in the system is zero in the cold phase and one in the hot phase.

The phase transition as a function of chemical potential extends to infinite temperature, where the vortex-vortex in-

*Electronic address: akao@math.ias.edu

 

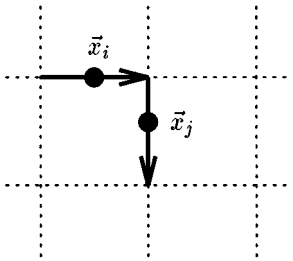


FIG. 1. Two vortex bonds with centers $\vec{x}_i$ and $\vec{x}_j$. The directions $\vec{\xi}_i$ and $\vec{\xi}_j$ are perpendicular.

teraction terms vanish. This polymeric limit of the vortex gas model can be related to the $XY$ model through a formalism entirely different from the spin-defect view. The Symanzik loop expansion of the $XY$ partition function expresses configurations in terms of collections of directed loops [29–31]. A chemical potential related to the spin-spin coupling controls the loop activity and there is no long-range interaction. The Symanzik loops can intersect, but repeated visits to a lattice site are suppressed. The polymeric limit of the vortex model is an approximation of the Symanzik model in which loop intersections are fully suppressed. It is believed that the critical behavior of single self-repelling loops is identical to that of single self-avoiding loops [32]. If penalized loop intersections are likewise irrelevant in the Symanzik form of the $XY$ model, so that the polymeric vortex transition is in the same universality class as the $XY$ ordering transition, then the long-range Biot-Savart interactions among vortices are also irrelevant at criticality.

The analysis of the polymeric model may be much simpler than theories of interacting vortices. Models of noninteracting vortex systems governed by a chemical potential [33,34] have been treated with transfer matrix and percolation theoretical techniques. Such techniques may be effective for the polymeric model of self-avoiding vortices also.

## II. SELF-AVOIDING-LOOPS MODEL

Individual vortices are oriented bonds on a periodic cubic lattice. The $i$th vortex has center $\vec{x}_i$ and direction $\vec{\xi}_i = \Gamma h \vec{e}$ where $\Gamma$ is a fixed circulation, $h$ is the lattice step size, and $\vec{e}$ is a unit vector in one of six signed coordinate directions. See Fig. 1. Let $L$ be the length of the cube, so a period contains $(L/h)^3$ sites. The present paper considers unit steps $h=1$.

The energy of a configuration of $N$ such vortices is given by

$$E = \nu N + \left[ \frac{1}{2} \sum_{i=1}^{N} \sum_{j \neq i} \vec{\xi}_i \cdot \vec{\xi}_j G(\vec{x}_i - \vec{x}_j) \right],$$

where $G(\vec{r})$ is the Green function for the Laplacian on the periodic cube. In free space, $G(\vec{r}) = 1/4\pi r$. The energy consists of a long-range vortex-vortex interaction term and a self-energy term, where $\nu$ is the self-energy of a vortex line of length $h$. The energy is a discretization of the Lamb integral for the kinetic energy of a smooth incompressible flow

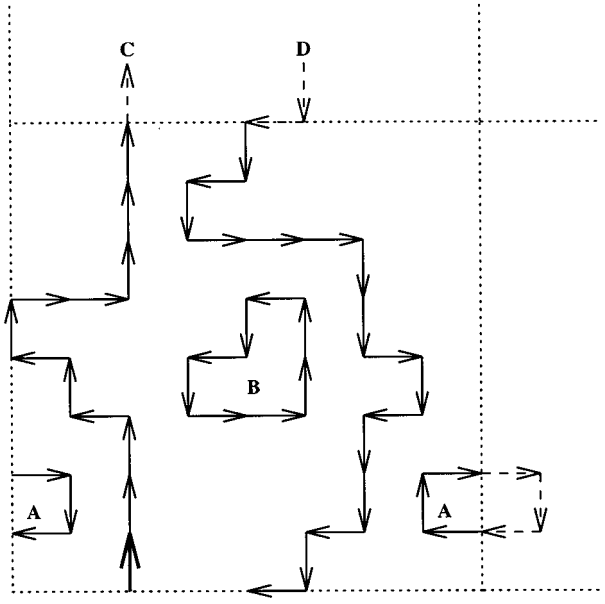


FIG. 2. Four schematic vortex loops in a periodic domain of length $L=8$. Loops $C$ and $D$ span the domain.

with vorticity $\vec{\xi} = \nabla \times \vec{u}$, where $\vec{u}$ is the fluid velocity [35], or equivalently, of the Biot-Savart energy of an electric current density $\vec{\xi}$:

$$E = \frac{1}{2} \int d\vec{x} \int d\vec{x}' \, \vec{\xi}(\vec{x}) \cdot \vec{\xi}(\vec{x}') G(\vec{x} - \vec{x}').$$

The circulation $\Gamma$ is set equal to 1 in the model studied here, while the parameter $\nu$ controls the vortex fugacity.

Vorticity configurations must be divergence free; at each lattice site the number of vortex bonds directed into the site must be equal to the number of vortex bonds directed out of the site. Vortex bonds therefore form collections of directed chains, which close into loops or extend to infinity.

In the model studied here, an additional constraint of self-avoidance is imposed so that each lattice site may have no more than one entering bond and one exiting bond. Forbidding multiple bond occupation imposes a cutoff on circulation density. Imposing the stronger constraint of self-avoidance should not change the large-scale physics, but has computational and formulational advantages. Configurations of self-avoiding chains of bonds are unambiguously partitioned into collections of separate directed self-avoiding walks. On the periodic lattice, each walk is closed and will henceforth be referred to as a vortex loop. Figure 2 shows four vortex loops in a periodic planar lattice.

Vortex configurations on the periodic lattice are taken to be neutral,

$$\sum_{i=1}^{N} \vec{\xi}_i = \vec{0},$$

so that the energy per unit volume is finite. The configurations correspond then to the vorticity of a periodic flow or to vortex defects in a periodic $XY$ spin system.

The configurations included in the thermodynamic ensemble comprise all arrangements of vortex bonds satisfying the aforementioned constraints of connectivity, self-avoidance, and neutrality. No constraint is imposed on the number of vortex links, on their distribution into loops, or on the topology of individual loops. Define $\Omega_2^{\rm SA}$ as the set of such loop configurations. Thermodynamic studies in which vortices remain connected into a single loop have been performed previously [8].

The Gibbs weight in the grand-canonical ensemble is

$$e^{-\beta E}=\exp\left\{-\beta\nu N-\beta\left[\frac{1}{2}\sum_{i=1}^{N}\sum_{j\neq i}\vec{\xi}_i\cdot\vec{\xi}_j G(\vec{x}_i-\vec{x}_j)\right]\right\}.$$

The principal thermodynamic quantities are the equilibrium energy per unit volume $E/V$, and the vortex line density $Nh/V$. The thermodynamic parameters are the inverse temperature $\beta$ and the vortex self-energy $\nu$. To better relate the simulation to other $XY$ representations, define a vortex activity parameter

$$\sigma=\beta\nu$$

and an interaction energy

$$E^{\rm int}=\frac{1}{2}\sum_{i=1}^{N}\sum_{j\neq i}\vec{\xi}_i\cdot\vec{\xi}_j G(\vec{x}_i-\vec{x}_j).$$

The partition function in $\beta$ and $\sigma$ is thus

$$\mathcal{Z}=\sum_{\Omega_2^{\rm SA}} e^{-\beta E}=\sum_{\Omega_2^{\rm SA}}\exp(-\sigma N-\beta E^{\rm int}).$$

A prime motivation for simulation in vorticity variables is to collect geometric information. Define the extent of a vortex loop containing $n$ bonds in the periodic domain as the side length of the smallest cube required to contain $n$ consecutive steps along the loop. In Fig. 2, loop A fits in a $2\times1(\times1)$ box, while loop B fits in a $2\times2(\times1)$ box. Both loops A and B thus have extent 2. Loop C has 12 bonds in the domain; following it for 12 steps traces an unclosed walk fitting in an $8\times2(\times1)$ box. Both loops C and D have extent 8. The equilibrium probability $p(n,s)$ of a bond being part of a loop of $n$ bonds and extent $s$ contains information on the geometry of vortices. One can also draw a parallel with percolation: define $\mathcal{P}$ as the probability of a configuration containing at least one loop with extent equal to or greater than the length of the domain. This is the analogue of the probability in percolation theory of an occupied cluster spanning the domain.

## III. RELATION TO THE *XY* MODEL

The ordering transition of the $XY$ model simulates the helium $\lambda$ transition. The $XY$ model is therefore an appropriate reference system for the vortex model. The self-avoiding-loops model is related to the three-dimensional $XY$ model both through a vortex-defect picture and through the Symanzik loop expansion. Consider the $XY$ partition function for a ferromagnetic coupling $K$:

$$\mathcal{Z}^{XY}=\sum_{\{\vec{S}\}}\exp\left(K\sum_{\langle i,j\rangle}\vec{S}_i\cdot\vec{S}_j\right).$$

Kohring and Shrock [36,24] counted the topological defects in the spin field to obtain the number of vortex bonds $N$ in a configuration. The vortex loops obtained by this process are not self-avoiding, but no two loops can share a bond (except for a set of measure zero). The vortex activity is offset in the Shrock model by a parameter $\lambda$:

$$\mathcal{Z}^{\rm KS}=\sum_{\{\vec{S}\}}\exp\left(K\sum_{\langle i,j\rangle}\vec{S}_i\cdot\vec{S}_j-\lambda N\right).$$

The Villian approximation can be used to decompose the spin energy into spin-wave and vortex terms:

$$-\sum_{\langle i,j\rangle nn}\vec{S}_i\cdot\vec{S}_j\approx E^{\rm spin\ wave}+c_1N+c_2E^{\rm int},$$

where $c_1$ and $c_2$ are positive constants. The self-avoiding loops model follows from the Shrock model by employing the approximation, discarding the spin-wave term, and replacing bond-avoiding vortex configurations with self-avoiding vortices. A change of variables $K=\beta/c_2$ and $\lambda=\sigma-c_1\beta/c_2$ then gives the self-avoiding-loops partition function:

$$\mathcal{Z}^{\rm SAL}=\sum_{\Omega_2^{\rm SA}}\exp(-\sigma N-\beta E^{\rm int}).$$

Setting $\beta=0$ to drop the interaction energy term gives the polymeric limit of the self-avoiding-loops model. The polymeric limit can also be related to the $XY$ model through the Symanzik loop expansion [29–31]. Consider configurations that consist of sets of closed, oriented, nearest-neighbor walks on the lattice. The walks need not be self-avoiding; for each lattice site $i$, denote the number of times any walk visits the site by $\tau_i$. Thus $\Sigma_i\tau_i$ is the total number of steps taken by all the walks in the configuration. Define $\Omega_2$ to be the set of all such configurations. The $XY$ model may be expressed as a gas of walks interacting only through a self-repelling contact interaction:

$$\mathcal{Z}^{XY}=\sum_{\Omega_2}\exp\left(-\sigma^*\sum_i\tau_i-\sum_i W(\tau_i)\right),$$

where $\sigma^*=-\ln(K)$, and where $W(\tau)$ is a weight function with $W(0)=W(1)=0$ and $W(\tau)\sim\tau\ln\tau$.

The weight function discourages multiple visits at any lattice site. If multiple visits are entirely forbidden, $W(\tau\geqslant2)=\infty$, then the configuration space is restricted to self-avoiding collections of walks. Steps can then be interpreted as ''vortices'' with $\Sigma_i\tau_i=N$. This restriction leads to the polymeric limit of the self-avoiding loops model, after formal substitution of $\sigma$ for $\sigma^*$:

$$\mathcal{Z}^{P}=\sum_{\Omega_2^{\rm SA}}\exp(-\sigma N).$$

Note that while the polymeric limit of the vortex model and the self-avoiding restriction of the Symanzik model have the same form, the former is a low-temperature approximation while the latter is a high-temperature expansion. As the ferromagnetic coupling $K$ increases, loop activity decreases in the vortex model while loop activity increases in the Symanzik model. The polymeric limit at criticality is thus in an approximate sense a self-dual representation of the three-dimensional $XY$ model.

## IV. SIMULATION OF SELF-AVOIDING LOOPS

The equilibria of the system are explored with a grand-canonical Monte Carlo simulation. Each configuration is stored as a collection of closed self-avoiding walks. Madras and co-workers have developed a set of transformations that modify the geometry of single self-avoiding walks [37,38]. These transformations are employed on random loops in the collection. The single-loop geometric updates are supplemented with transformations that change the loop connectivity: joining two separate loops or breaking a single loop apart. Transformations are also employed to add or delete vortex bonds from the configuration. Metropolis-type rejection is used to enforce the Gibbs weight.

The direct simulation of interacting vortices is for several reasons less efficient than simulation of spins. The first drawback is that a complex set of transformations and data structures is required to operate on the configurations in such a way as to preserve the constraints. A second drawback is that the computation of the energy requires on the order of $N^2$ operations for a configuration of $N$ vortices. The computational effort in computing the energy thus scales with the square of the volume of the system, or with the sixth power of the length of the system. The increase of autocorrelation times with the system size compounds the problem. For these reasons only relatively small systems are simulated. Most of the data are taken for domains of length 4, 6, and 8. Spot checks are conducted on domains of length 16. The data are thus suitable for determining the overall thermodynamic behavior of the system, but are not accurate enough for the computation of critical exponents. Such values may be better obtained by analytical means.

Thermodynamic data are computed with the histogram method of Ferrenberg and Swendsen [39]. The histograms are taken in bins over the interaction energy $E^{\mathrm{int}}$, the number of vortex bonds $N$, and the existence of a loop spanning the domain. Histogram merger and histogram shifting techniques allow the thermodynamic observables to be computed as functions of the parameters $\beta$ and $\sigma$. Loop geometry information $p(n,s)$ is collected without histograms.

The use of the histogram methods makes an estimate of the statistical error very complicated. Each point of a graph is computed with data from several runs taken at different parameter values, which thus have different autocorrelation times. Errors are subjectively controlled by taking data until the histograms become fairly smooth, and by determining the effect of adding more data in batches. The alignment of thermodynamic features in the $\beta,\sigma$ plane for different system sizes is taken as an indication that statistical errors are not excessive.

The Monte Carlo algorithm is fully described in [40,41].

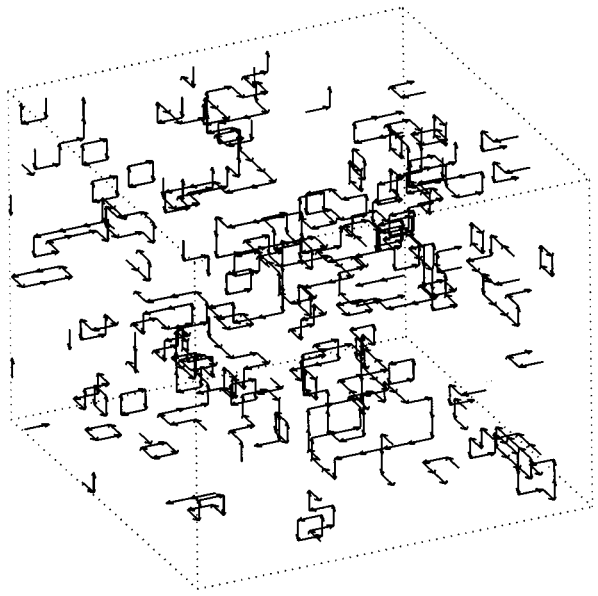

FIG. 3. Example vortex configuration containing 76 loops from simulation at $L=16$. A single period of the domain is shown.

## V. SIMULATION RESULTS

Figure 3 shows a collection of vortex loops on a periodic lattice of side length 16. Loops containing few bonds are more common than loops containing many bonds, and large loops typically have a complex, tangled structure.

The simulation identifies a percolation threshold in the $\beta$, $\sigma$ plane. In the region identified as phase II, the cold phase, in Fig. 4 there are no vortex loops of infinite extent in an infinite system. In the region identified as phase I, the hot phase, there is almost certainly an infinite vortex loop in an infinite system. The dotted line indicates the location of a

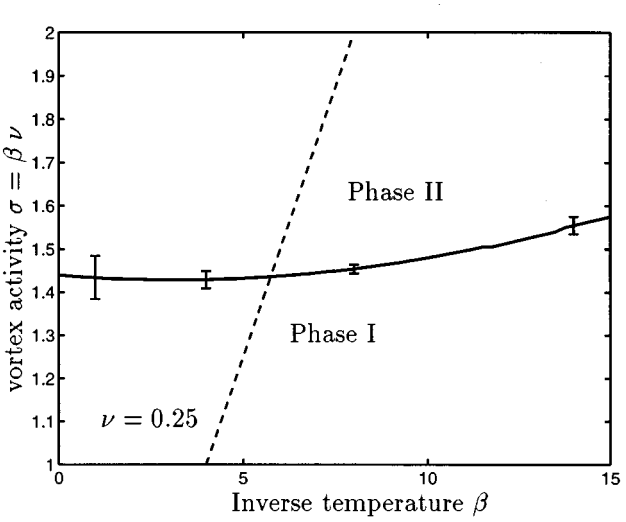


FIG. 4. Phase plane in $(\beta,\sigma)$. The solid line marks the transition between phase II, the ''superfluid'' phase, and phase I, the ''normal'' phase. The dashed line through the transition is the curve of constant vortex self-energy $\nu=0.25$. Error bars are drawn at arbitrary locations on the transition curve.

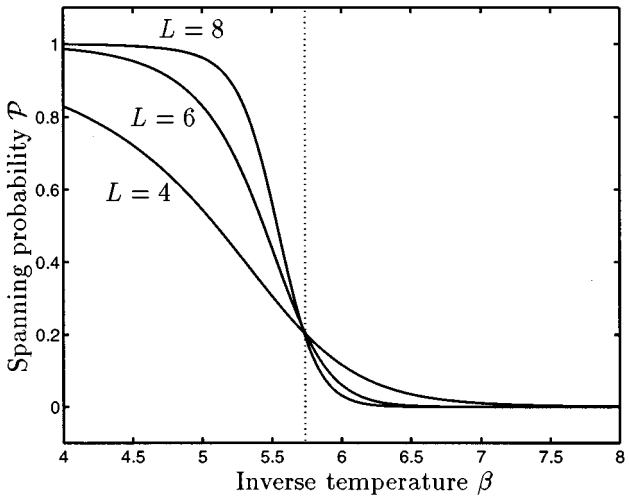


FIG. 5. Probability $\mathcal{P}$ that a loop spanning the domain exists at inverse temperature $\beta$ and fixed loop self-energy $\nu = 0.25$. Solid curves are data for system sizes $L = 4$, $L = 6$, and $L = 8$. The threshold location $\beta_c(\nu = 0.25) = 5.74$ is marked with a dotted line.

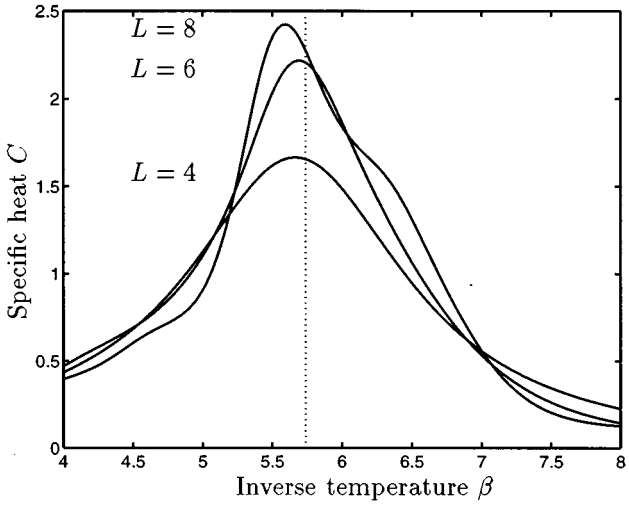


FIG. 6. Specific heat at inverse temperature $\beta$ and fixed loop self-energy $\nu = 0.25$. Solid curves are data for system sizes $L = 4$, 6, and 8. The threshold location $\beta_c(\nu = 0.25) = 5.74$ is marked with a dotted line.

slice of constant vortex self-energy $\nu = 0.25$.

The location of the threshold is identified by the finite size scaling of the probability $\mathcal{P}$ of the existence of a vortex loop spanning the system. Figure 5 shows a slice through the threshold at $\nu = 0.25$. For values of the inverse temperature $\beta$ less than the critical temperature marked with a dotted line, the percolation probability increases as the system size increases. For values of $\beta$ greater than the critical value, the probability decreases as the system size increases. This finite size scaling indicates the presence of a percolation threshold [42]: on one side of the threshold an infinite vortex exists with probability one in an infinite system, while on the other side there is almost certainly no infinite vortex. This behavior supports the conjecture, of Feynman and Onsager [12], that an infinite tangle of thermally excited vorticity appears at the λ transition. The subjective error bars in Fig. 4 are based primarily on the agreement of the crossing points of the percolation curves for the three system sizes.

The finite size scaling of the thermodynamic quantities indicates the presence of a phase transition coincident with the percolation threshold. Figure 6 shows the specific heat

$$C = \frac{-\beta^2}{V} \frac{\partial E}{\partial \beta}$$

in relation to the threshold temperature marked with the dotted line. The height of the peak increases with the system size, indicating a divergence or a cusp in the thermodynamic limit. The value of the energy,

$$E = \nu N + E^{\text{int}},$$

shown in Fig. 7, shows no dependence on the system size, indicating that the energy is continuous at the transition point. This thermodynamic behavior is compatible with the λ transition.

Statistical error is evident in the specific heat curve for the largest system, $L = 8$, but it retains the highest peak all along the transition line. The percolation threshold is shown along with the location of the $L = 6$ specific heat peak in Fig. 8. The subjective error bars are based on the spread of the peak locations and incorporate both statistical error and finite size shifting.

The appearance of an infinite loop at the transition is a true percolation phenomenon, and is not due to any jump in the density of vortex bonds. See Fig. 9. The threshold occurs at a fixed density, which varies from approximately $D = 0.15$ at $\beta = 0$ to $D = 0.4$ at $\beta = 15$.

The simulation data can be further compared to percolation problems by examining the analogue of cluster numbers. Figure 10 plots the probability $p(n)$ of a bond being part of

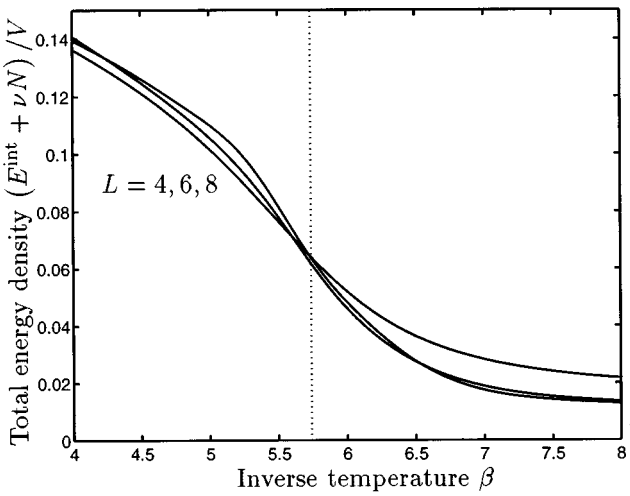


FIG. 7. Total energy $E^{\text{int}} + \nu N$ per lattice site at inverse temperature $\beta$ and fixed loop self-energy $\nu = 0.25$. Solid curves are data for system sizes $L = 4$, 6, and 8. The threshold location $\beta_c(\nu = 0.25) = 5.74$ is marked with a dotted line. System size dependence is not significant.

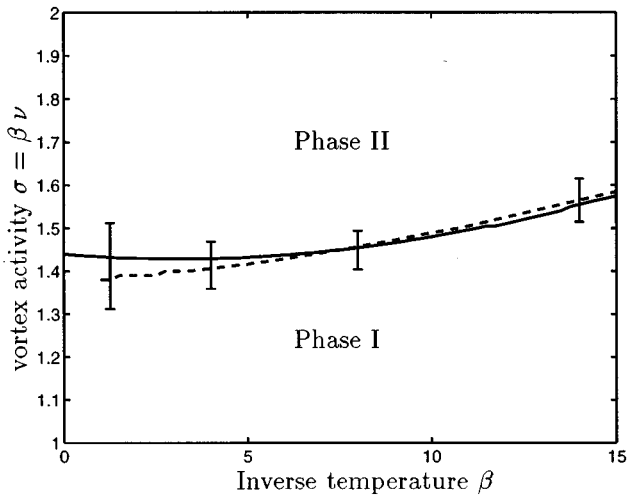


FIG. 8. Locations of the percolation threshold and the peak of the specific heat in the $(\beta,\sigma)$ plane. The solid line is the percolation threshold and the dashed line is the peak location of the specific heat at $L=6$. The lines separate the ''superfluid'' phase, phase II, from the ''normal'' phase, phase I. Arbitrarily placed error bars indicate both statistical and finite size uncertainties in the transition location.

a loop of $n$ bonds. The graphs are normalized by the probability $p(4)$ of a bond being contained in a loop of the smallest size. Line $A$ is from the cold phase, line $B$ is at criticality, and line $C$ is above criticality at infinite temperature. The probabilities appear to have an exponential decay in $n$ in the cold phase, while the decay seems to follow a power law at and above the transition at which a loop spanning the domain appears. A fit to lines $B$-$D$ for $n \leqslant 60$ gives the scaling

$$p(n) \propto n^{-1.7\pm0.1}.$$

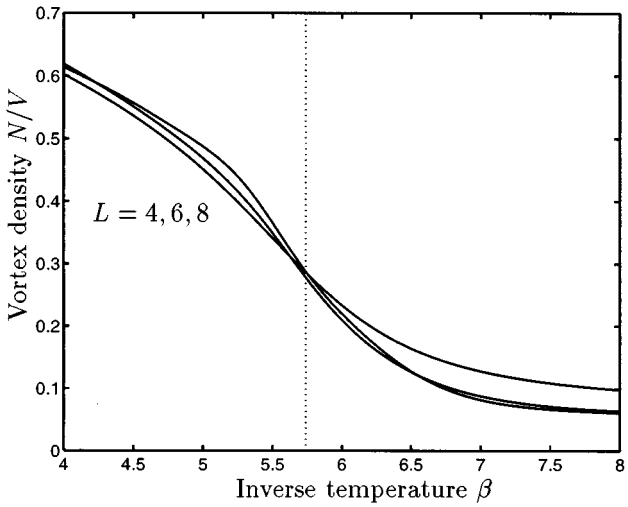


FIG. 9. Number of vortex bonds $N$ per lattice site at inverse temperature $\beta$ and fixed loop self-energy $\nu=0.25$. Solid curves are data for system sizes $L=4$, 6, and 8. The threshold location $\beta_c(\nu=0.25)=5.74$ is marked with a dotted line. System size dependence is not significant.

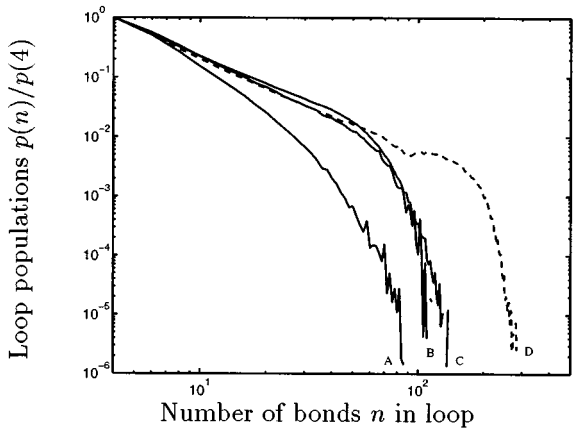


FIG. 10. Loop populations $p(n)/p(4)$ by number of bonds $n$. The probability that a bond is part of a loop of $n$ bonds is $p(n)$. The smallest loops have $n=4$. Solid lines $A$, $B$, and $C$ are from system size $L=8$ and represent the cold phase, criticality, and the hot phase, respectively. Dashed line $D$ is at criticality for $L=16$ and delineates a dropoff due to finite size effects.

The first three lines are taken at system size $L=8$, while line $D$ is at criticality for $L=16$. The $L=16$ data indicate that the final dropoff at large $n$ is due to finite size effects. The data confirm the overall behavior of the populations of loops of $XY$ vortex defects in the study by Epiney [25].

## VI. DISCUSSION AND CONCLUSIONS

The simulation of the vortex system indicates the existence of a λ-like phase transition in a model with a simplified vorticity based Hamiltonian. The transition is furthermore shown to coincide with a percolation threshold for vortex loops. The threshold extends to infinite temperature, where the vortex-vortex interactions vanish and the model becomes a gas of oriented polymers.

Two mechanisms may contribute to the nonanalyticity of the energy $E=\sigma N+E^{\rm int}$ at the threshold. The first is independent of the interaction energy and is due to nonanalyticity of the vortex bond density across the percolation threshold. Such behavior is not present in independent bond percolation, but arises from the effects of connectivity and self-avoidance constraints on configurations in $\Omega_2^{\rm SA}$. Nonanalyticity in a vortex system with geometric constraints also exists in models studied by King and co-workers [33,34].

A second mechanism depends on the interaction energy, and is due to the possible appearance of long-range order in the vortex bond directions at the percolation threshold. Above the transition temperature, a nonzero fraction of bonds are contained in infinite self-avoiding walks. Single oriented self-avoiding walks have been shown to have vector-vector correlations with power-law decay [43]. It is conceivable that while bond directions in separate vortex loops of finite extent become exponentially decorrelated at distances much larger than the loop size, bond directions in infinite loops may have power-law correlations. One should note, however, that the presence of a gas of loops may change the statistics of the infinite walks. de Gennes has conjectured that a self-avoiding walk in a gas of other walks

behaves like the simple random walk [44]. Polarization effects between loops of different scale may also need to be taken into account.

The phase diagram of the self-avoiding loops model is consistent with the equivalent portion of the ordering transition in the Shrock extension of the $XY$ model. The infinite temperature transition point in the vortex system at $\sigma_c \approx 1.4$ is not the same as the infinite temperature transition point in the spin system at $\lambda_c \approx 0.55$, but the replacement of bond-avoiding vortices with fully self-avoiding vortices is expected to change the transition location. A calculation of critical exponents is required to verify that the self-avoiding loop and the $XY$ vortex models lie in the same universality class.

This simulation is not accurate enough for direct computation of critical exponents, but the results may be applied to vortex theories in a number of ways. A percolation theoretical analysis could give exponents for the entropy driven activity of finite size loops and for the strength of the percolating loop near the transition. The observed scaling of $p(n)$ could be used to aid the analysis. These exponents could be combined with an ansatz for the interaction energy of loops of a given scale [16] to compute exponents for the vortex system.

The existence of long-range ordering of vortex bonds at the transition remains an open question. If vortices do not order, the speculation that the polymeric model and the $XY$ model lie in the same universality class would be supported. Such a result could also lead to verification that $\phi^4$ and $N$-vector models lie in the same universality class [45]. Even if long-range interactions are relevant at criticality, the polymeric model may serve as a base for an expansion viewing the interaction energy coefficient as a small parameter. One would ultimately expect, however, that long-range interactions remain important for understanding dynamic problems of superfluid flow away from the $\lambda$ transition.

## ACKNOWLEDGMENTS

The author wishes to thank Alexandre Chorin for advice and assistance in this effort, and Thomas Spencer for pointing out the connection to the loop expansion. The author gratefully acknowledges the support of the Sloan Foundation, of the Applied Mathematical Sciences Subprogram of the Office of Energy Research, U.S. Department of Energy under Contract No. DE-AC03-76SF00098, of the National Science Foundation Grant No. DMS-9407480, and of NEC Research Institute, Inc.

[1] C. F. Barenghi, R. J. Donnelly, and W. F. Vinen, J. Low Temp. Phys. **52**, 189 (1983).
[2] D. R. Tilley and J. Tilley, *Superfluidity and Superconductivity* (Bristol, Boston, 1986).
[3] E. Varoquaux, G. G. Ihas, O. Avenel, and R. Aarts, J. Low Temp. Phys. **89**, 207 (1992).
[4] A. J. Chorin, *Vorticity and Turbulence* (Springer, New York, 1993).
[5] M. Lesieur, *Turbulence in Fluids: Stochastic and Numerical Modelling*, 2nd ed. (Kluwer Academic Publishers, Boston, 1990).
[6] Z. She, E. Jackson, and S. Orszag, Nature **344**, 226 (1990).
[7] W. D. McComb, *The Physics of Fluid Turbulence* (Oxford, New York, 1990).
[8] A. J. Chorin, Commun. Math. Phys. **141**, 619 (1991).
[9] D. Montgomery and G. Joyce, Phys. Fluids **17**, 1139 (1974).
[10] R. Robert and J. Sommeria, J. Fluid Mech. **229**, 291 (1991).
[11] J. Miller, P. B. Weichman, and M. C. Cross, Phys. Rev. A **45**, 2328 (1992).
[12] R. P. Feynman, in *Progress in Low Temperature Physics*, edited by C. J. Gorter (North-Holland, Amsterdam, 1955).
[13] C. Dasgupta and B. I. Halperin, Phys. Rev. Lett. **47**, 1556 (1981).
[14] S. R. Shenoy, Phys. Rev. B **40**, 5056 (1989).
[15] G. A. Williams, J. Low Temp. Phys. **89**, 91 (1992).
[16] A. J. Chorin and O. H. Hald, Phys. Rev. B **51**, 11 969 (1995).
[17] J. Kosterlitz and D. J. Thouless, J. Phys. C **6**, 1181 (1973).
[18] J. Frohlich and T. Spencer, Commun. Math. Phys. **81**, 527 (1971).
[19] M. E. Fisher, X. J. Li, and Y. Levin, J. Stat. Phys. **79**, 1 (1995).
[20] A. J. Chorin, J. Stat. Phys. **76**, 835 (1994).
[21] J. C. Le Guillou and J. Zinn-Justin, Phys. Rev. B **21**, 3976 (1980).
[22] R. Savit, Rev. Mod. Phys. **52**, 453 (1980).
[23] J. V. Jose, L. P. Kadanoff, S. Kirkpatrick, and D. R. Nelson, Phys. Rev. B **16**, 1217 (1977).
[24] G. Kohring and R. Shrock, Nucl. Phys. B **288**, 397 (1987).
[25] J. Epiney, Interdisciplinary Project Center of Supercomputing, ETH-Zentrum CH-8092 Zurich Technical Report No. 90-08 (unpublished).
[26] P. B. Weichman, Phys. Rev. Lett. **61**, 2969 (1988).
[27] D. R. Nelson and R. D. Kamien, J. Stat. Phys. **71**, 23 (1993).
[28] B. I. Halperin and D. R. Nelson, J. Low Temp. Phys. **36**, 594 (1979).
[29] R. Fernandez, J. Frohlich, and A. D. Sokal, *Random Walks, Critical Phenomena, and Triviality in Quantum Field Theory* (Springer, New York, 1992).
[30] D. C. Brydges, J. Frolich, and T. Spencer, Commun. Math. Phys. **83**, 123 (1982).
[31] K. Symanzik, in *Local Quantum Theory*, edited by R. Jost (Academic, New York, 1969).
[32] N. Madras, *The Self-avoiding Walk* (Birkhauser, Boston, 1993).
[33] C. Borgs, J. T. Chayes, and C. King, J. Phys. A **28**, 6483 (1995).
[34] C. King (unpublished).
[35] A. J. Chorin, Commun. Math. Phys. **132**, 519 (1990).
[36] G. Kohring, R. E. Shrock, and P. Wills, Phys. Rev. Lett. **57**, 1358 (1986).
[37] N. Madras and A. D. Sokal, J. Stat. Phys. **50**, 109 (1988).
[38] N. Madras, A. Orlitsky, and L. A. Shepp, J. Stat. Phys. **58**, 159 (1990).
[39] A. M. Ferrenberg and R. H. Swendsen, Phys. Rev. Lett. **63**, 1195 (1989).
[40] J. H. Akao, Ph.D. thesis, University of California at Berkeley, 1994 (unpublished).

[41] J. H. Akao (unpublished).
[42] D. Stauffer and A. Aharony, *Introduction to Percolation Theory*, 2nd ed. (Taylor and Francis, London, 1994).
[43] A. J. Chorin and J. H. Akao, Physica D **52**, 403 (1991).
[44] P. G. de Gennes, *Scaling Concepts in Polymer Physics* (Cornell University Press, Ithaca, 1979).
[45] C. Aragao De Carvalho, S. Caracciolo, and J. Frohlich, Nucl. Phys. B **215**, 209 (1983).